Delamination Damage Propagation Behavior of Composite Laminate Plate Under Low-Velocity Impact Using a New Adhesive Layer Model

Y. ZHAO, *K. DONG, Y. GAO

School of Naval Architecture and Ocean Engineering, Harbin Institute of Technology AT WeiHai, Weihai 264209, Shandong P.R. China

*Corresponding author: dongke213@126.com

Abstract

Based on interface adhesive theory and delamination damage mechanism, a new adhesive layer model is proposed to analyze the intra-layer delamination damage process of composite laminated plate subjected to low velocity impact. The influences of through-thickness tensile stresses, inter-laminar shear stresses and matrix cracking on delamination damage are taken into consideration in this model. Compared with traditional strength failure criterion model or fracture mechanics energy release rate model, analytical results of this model are in good agreement with experimental data. The damage extension characteristics and the various influence factors on delamination damage are discussed. The results of this research can be applied in composite structure design and life prediction.

Keywords: composite laminated plate; delamination damage; adhesive layer model; damage extension characteristics

1. Introduction

Composite laminates are being increasingly used in aerospace, automotive, shipbuilding and other industries fields due to their inherently high specific mechanical properties. In those service conditions, transverse impact at low velocity is the normal form of loading which can cause internal damage such as delamination, matrix cracking, local permanent deformationand fiber breakage, leading to a reduction of load carrying capacity of the composite structures. Furthermore, catastrophic failure may occur when the composite laminates are serviced in such damaged state. Hence, understanding the damage involved in the impact of composite targets is important in the effective design of a composite structure.

However, the dynamic behavior of composite laminates is very complex, because there are many concurrent phenomena during composite laminate failure under impact load. The inherent complexity of the structure of composite has brought great difficulties to the experimental or theoretical methods. With the development of numerical techniques, numerical analysis based on finite element method has been widely used in recent years, and many efficient numerical models have been made to analyze the impact problem. Based on continuum damage mechanics, Matzenmiller (1995) first brought up CDM concept which links up the composite material damage and degradation of the elastic properties of materials. This method shows a good prediction of the impulse response of laminates and the damage layer, but can’t be predicted the fiber breakage and damage of the matrix damage accurately. Hou(2000), based on strength theory, studied the low speed dynamic response and damage modes by using explicit finite element algorithm. At the same time the material parameters degradation is replaced by the stress degradation and stiffness degradation. Zerbst(2009) introduced the fracture mechanics methods to predict composite laminates residual compressive strength and delamination damage, but this method can't accurately predict the delamination area.

Considering the disadvantages of present method, this paper proposes a new adhesive layer model is proposed to analyze the intra-layer delamination damage process of composite laminated plate subjected to low velocity impact based on interface adhesive theory and delamination damage mechanism. The influences of through-thickness tensile stresses, inter-laminar shear stress and matrix cracking on delamination damage are taken into consideration in this model. Compared with traditional strength failure criterion model or fracture mechanics energy release rate model, analytical results of this model are in good agreement with experimental data. The damage extension characteristics on delamination damage are discussed. The results of this research can be applied in composite structure design and life prediction..

2. Impact damage constitutive model

2.1 Three-dimensional rate-dependent constitutive model

Assuming the fiber as the uniform transversely isotropic linear elastic body and the matrix as isotropic viscoelastic, Kairm (2005) derived the expression of the relaxation modulus of this materials under high strain rate:

$$\left.\begin{aligned} E_{11}(t) &= (E_{f1}V_f + E_m V_m) + E_1 V_m e^{-\frac{1}{\theta_{e1}}} + E_2 V_m e^{-\frac{1}{\theta_{e2}}} \\ E_{22}(t) &= \frac{E_{f2}E_m}{E_{f2}V'_m + E_m V'_f} + Qe^{-Mt} + \mathrm{Re}^{-Nt} \\ G_{12}(t) &= \frac{G_{f12}G_m}{G_{f12}V'_m + G_m V'_f} + Q_{12}e^{-M_{12}t} + R_{12}e^{-N_{12}t} \\ G_{23}(t) &= \frac{G_{f23}G_m}{G_{f23}V'_m + G_m V'_f} + Q_{23}e^{-M_{23}t} + R_{23}e^{-N_{23}t} \end{aligned}\right\} \tag{1}$$

Based on the Hooke's law, the constitutive model can be expressed as:

$$\varepsilon = S\sigma = EU\sigma \tag{2}$$

Where E is stiffness matrix, S is compliance matrix. The expression of U is

$$U = \begin{bmatrix} 1 & -\mu_{12} & -\mu_{31} & 0 & 0 & 0 \\ -\mu_{12} & 1 & -\mu_{23} & 0 & 0 & 0 \\ -\mu_{31} & -\mu_{23} & 1 & 0 & 0 & 0 \\ 0 & 0 & 0 & 1 & 0 & 0 \\ 0 & 0 & 0 & 0 & 1 & 0 \\ 0 & 0 & 0 & 0 & 0 & 1 \end{bmatrix} \tag{3}$$

Considering the 2 and 3 direction of the unidirectional fiber-reinforced composite material having the same mechanical properties, so the three-dimensional constitutive relation can be expressed as:

$$\begin{Bmatrix} \sigma_{11} \\ \sigma_{22} \\ \sigma_{33} \\ \sigma_{12} \\ \sigma_{23} \\ \sigma_{31} \end{Bmatrix} = U^{-1} \begin{Bmatrix} \int_0^t E_{11}(t-\tau)\dot{\varepsilon}(\tau)d\tau \\ \int_0^t E_{22}(t-\tau)\dot{\varepsilon}(\tau)d\tau \\ \int_0^t E_{22}(t-\tau)\dot{\varepsilon}(\tau)d\tau \\ \int_0^t E_{12}(t-\tau)\dot{\varepsilon}(\tau)d\tau \\ \int_0^t E_{23}(t-\tau)\dot{\varepsilon}(\tau)d\tau \\ \int_0^t E_{12}(t-\tau)\dot{\varepsilon}(\tau)d\tau \end{Bmatrix} \tag{4}$$

2.2 The material failure criterion and the stiffness reduction scheme

The research of the inner-layer damage of composite material mainly includes three parts: the calculation of stress or strain, the criteria of the damage failure and the degradation of material properties. On the failure criteria of composite material, the improved Chang / Chang failure criteria (Hou, 2000) is used as the criteria of the inner-layer damage in this paper:

Fiber tensile failure mode: $$F_{fiber} = \left(\frac{\delta_1}{s_1}\right)^2 + \bar{\tau} > 1 \tag{5}$$

Matrix cracking failure mode: $$F_{matrix} = \left(\frac{\delta_2}{S_2}\right)^2 + \bar{\tau} > 1 \tag{6}$$

Matrix compressive failure mode:

$$F_{comp} = \left(\frac{\delta_2}{2s_{12}}\right)^2 + \left[\left(\frac{c_2}{2s_{12}}\right)^2 - 1\right]\frac{\delta_2}{c_2} + \bar{\tau} > 1 \tag{7}$$

$$\bar{\tau} = \frac{\frac{\tau_{12}^2}{2G_{12}} + \frac{3}{4}\alpha\tau_{12}^4}{\frac{S_{12}^2}{2G_{12}} + \frac{3}{4}\alpha S_{12}^4} \tag{8}$$

The mechanical properties must be decreased in damaged areas. In order to make sure the accuracy of the simulation, the stiffness of the laminate is reduced step by step. Different forms of the reduction scheme of material stiffness are applied depending on the form of damage. When the failure happens, the repeated degradation method will be taken (Sebastian, 2008), the degradation scheme is as follows:

Table 1. Stiffness reduction scheme

Failure mode	Parameter reduction
Fiber tensile	$E_{11} = E_{22} = G_{12} = \upsilon_{21} = \upsilon_{12} = 0$
Matrix cracking	$E_{22} = \upsilon_{21} = 0,\ G_{12} = 0$
Matrix compressive	$E_{11} = \upsilon_{21} = \upsilon_{12} = 0, G_{12} = 0, X_C = 2Y_C$

2.3 Interface cohesive element damage model

The interface cohesive element is introduced into the low speed impact process of composite laminates in this paper. A three-dimensional interface cohesive element (Fig1) is adopted to study the delamination damage. Biphasic constitutive relation of interface element is used to describe the initiation and progression of crack. When the relative displacement of interface element δ is less than δ^0, no damage occurs. It is shown in the interface strength -relative displacement curve that the slope is the interface element stiffness. When the relative displacement is more than δ^0, interface element damage occurs and the interface element stiffness begins to gradually decrease. The new interface stiffness curve is shown in figure 2 with dotted line. With the continual progression damage of the interface element, the relative displacement increases and the interface unit will be completely destroyed. Then the interface element stiffness becomes zero. The area formed by O, A, B three points is energy release rate in the process of damage of the interface element. The initial damage criteria of the model is shown as follows:

$$\left(\frac{T_N}{T}\right)^2+\left(\frac{S_1}{S}\right)^2+\left(\frac{S_2}{S}\right)^2=1 \qquad T_N\geq 0 \tag{9}$$

$$\left(\frac{S_1}{S}\right)^2+\left(\frac{S_2}{S}\right)^2=1 \qquad T_N<0 \tag{10}$$

where: $\delta^0=\delta_{\mathrm{I}}{}^0\delta_{\Pi}{}^0\sqrt{\dfrac{1+\beta^2}{\left(\delta_{\Pi}{}^0\right)^2+\left(\beta\delta_{\mathrm{I}}{}^0\right)^2}}$; $\delta_{\mathrm{I}}{}^0=\dfrac{T}{EN}$, $\delta_{\Pi}{}^0=\dfrac{S}{ET}$; $\beta=\dfrac{\delta_{\mathrm{I}}}{\delta_{\Pi}}$

The formula of final failure displacement of the mixed-mode is:

$$\delta^f=\begin{cases}\dfrac{2(1+\beta)^2}{\delta^0}\left[\left(\dfrac{EN}{GIC}\right)^{XMU}+\left(\dfrac{ET\cdot\beta^2}{G\Pi C}\right)^{XMU}\right]^{-\frac{1}{XMU}} & \ldots(XMU>0)\\ \dfrac{2}{\delta^0\left(\dfrac{1}{1+\beta^2}EN+\dfrac{\beta^2}{1+\beta^2}ET\right)}\left[GIC+(G\Pi C-GIC)\left(\dfrac{\beta^2\cdot ET}{EN+\beta^2 ET}\right)^{|XMU|}\right] & \cdots(XMU<0)\end{cases} \tag{11}$$

With the continuous development of damage, a macroscopic crack appears in the interface. It is similar to the crack development in the fracture mechanics. Therefore, the criterion of the rate of strain energy release in fracture mechanics can be used for the analysis of interface crack progression. And the criteria of the damage progression is shown as follows:

$$\left(\frac{G_{\mathrm{I}}}{G_{\mathrm{I}C}}\right)^2+\left(\frac{G_{\Pi}}{G_{\Pi C}}\right)^2+\left(\frac{G_{\mathrm{III}}}{G_{\mathrm{III}C}}\right)^2=1 \tag{12}$$

where G_{I} 、 G_{Π} 、 G_{III} respectively mean the rate of strain energy release of the normal and two tangential of the interface element; $G_{\mathrm{I}C}$、$G_{\mathrm{II}C}$、$G_{\mathrm{III}C}$ respectively mean the critical energy release rate of Ⅰ, Ⅱ, Ⅲ crack interface models.

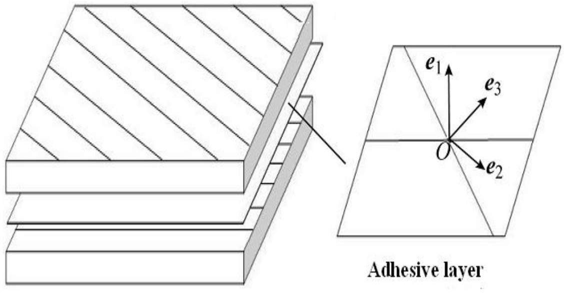

Fig.1 Mechanics model of the laminates

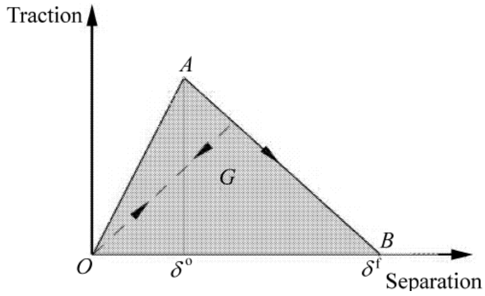

Fig.2 Interface force-relative displacemen

3. The finite element model

3.1 Material model and boundary conditions

Composite material is continuous unidirectional tensile high-strength Carbon fibers (Tenax HTS40 12 K 300). The thickness of composite laminate plate is 2 mm with a ply thickness of 0.25 mm in a staking sequence $[0/90]_{2S}$. The laminate plate is fixed by a rigid fixture and a diameter of 75 mm circular preformed hole is reserved. The material performance of the interface layer has a great impact on delamination damage (Masaaki, 2007). Therefore, its performance parameters are generally measured by the method of experiment. The parameters used in the paper are got from Shi's (2012) experimental data. The materials of impactor and fixtures are steel. Material parameters taken as follows: E=210 Gpa; ρ=7850 kg/m^3; ν=0.3. The diameter of impactor is 15 mm. The impact velocity is 3.83 m/s. The impact energy is 7.35 J. Considering that the stiffness of steel is relatively larger than the stiffness of laminate plate, so the impactor and clamp are defined as the rigid body.

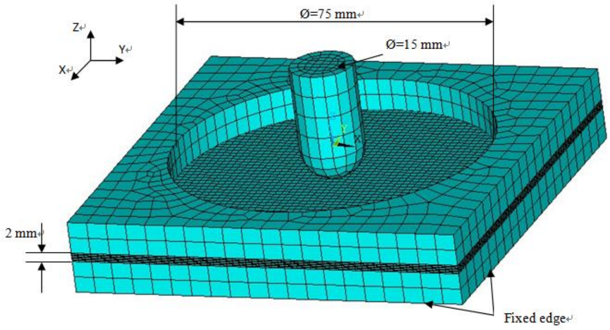

Fig. 3 Finite element model

3.2 Types of element used in coupled numerical model

Considering the importance of delamination damage under the low velocity impact, two kinds of elements are chosen: Each ply of Laminate plate uses 3D solid elements, which not only can consider the stress in thickness direction of laminate plate, but also can consider the effect of nonlinear shear. At the same time, we introduce a layer of 3D solid shell elements sub-layers between upper layer and lower layer of laminate plate which shown in Fig 1, it makes sure the displacement continuity of the structure. The advantage of 3D solid shell elements is that it can simulate a larger length to thickness ratio of element and has a fast calculation. It also needn't to use the mass scaling.

3.3 Contact algorithm

The material properties of impactor, fixtures and laminate plate have great different. Between the impactor and the sub-layer, as well as the fixtures and the sub-layer， based on the contact segment, the automatic algorithm is established. This contact algorithm does not depend on the material parameters, but the quality of the node divied by the square of the time step size, which can guarantee the stability and reliability of computation. A kind of tied contact is used between the upper and lower surfaces of interface element contact with adjacent sub-layer respectively. The benefit of tied connect is bounding the slippage of the adhesive layer on upper and lower of sub-layer, which is more in accord with the real structure mechanism of laminated plate. In order to prevent penetration between sub-layer, the automatic contact is established in each ply.

Coefficient of friction between the object depends on the material properties and surface smoothness, coefficient of friction measured experimentally is more accurately. The existing research results of predecessors show that the friction coefficient has a great influence on the impact test, especially on the absorption of impact energy (Schon, 2000). Considering the adhesive effect between the adhesive layer and the sub-layers, the friction coefficient takes a relatively large value of 0.5, at the rest of contact take a value of 0.3.

4. Results and discussion

In order to verify the calculated feasibility and accuracy, the simulation results are compared with experimental results which shown in Fig. 4. One can see that the two results from two different solving methods are nearly in agreement. It is also seen from Fig. 4(a) that impact force in the times interval of 0ms to approximate 0.7ms increases approximately linearly, it meanwhile laminated plate material is in the elastic deformation stage, in other word, the damaged does not appear. The damage occurs within laminates when the times form 0.6ms to the peak value1.6ms. After the peak impact force, the impactor begins to rebound until the impact force to zero. Compared to the peak time which shown in Fig. 4a (approximate 1.6ms), the impact energy peak time which shown in Fig. 4b (approximate 2.0ms) appears later. The

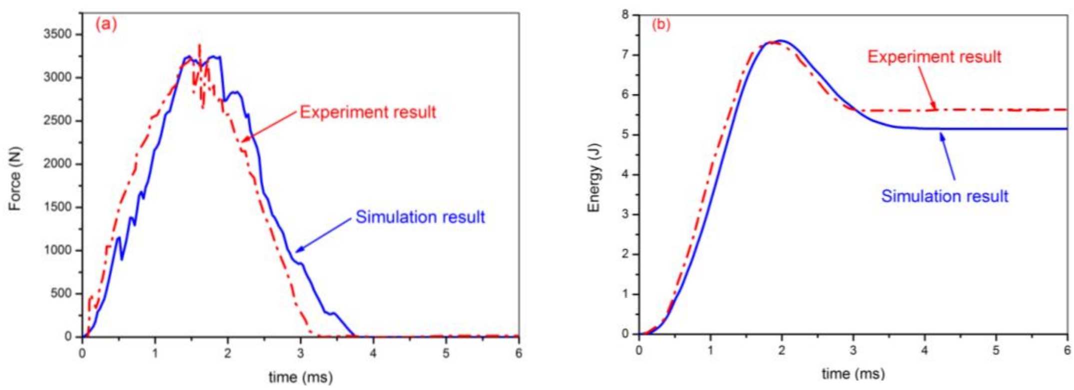

Fig.4 Dispersion curves of low-velocity impact with two different methods

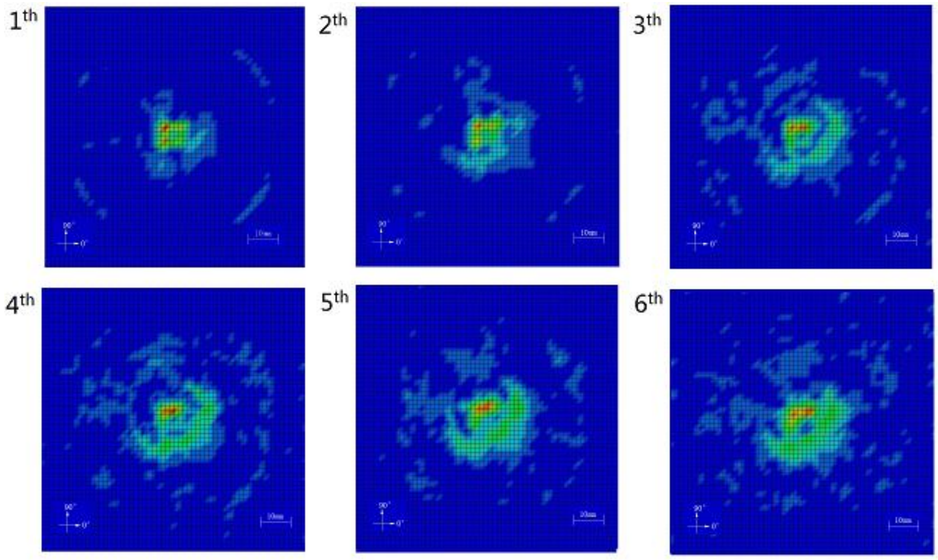

Fig.5 The stress clouds in different cohesive layers

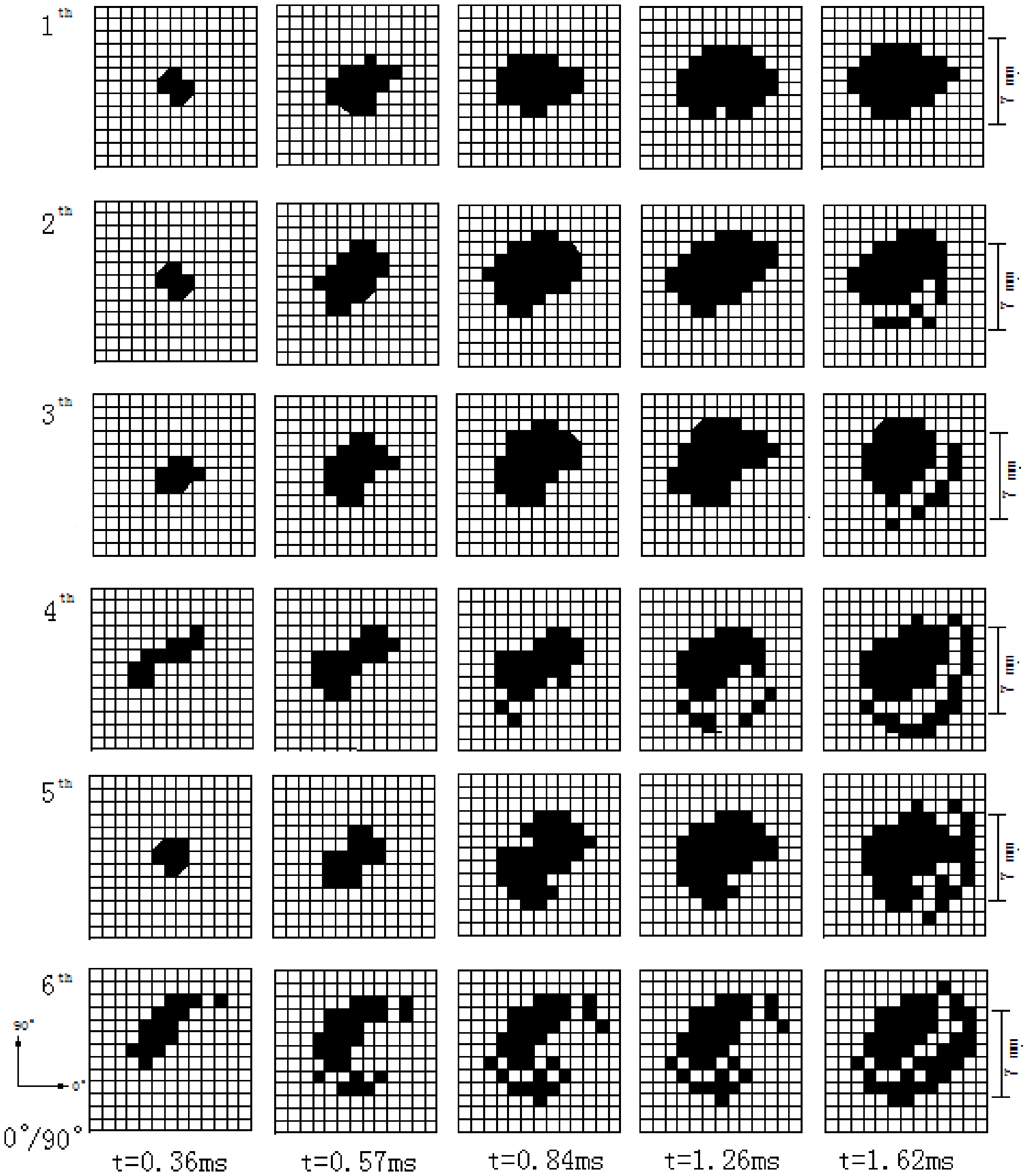

Fig.6 Delamination damage growth images in adhere layers

reason causing this kind of phenomenon is the impact energy continue increase when the impact force reachs its maximum value.

Once impactor contacts laminated plate, part of the energy will be absorbed by elastic deformation, the other energy will be dissipated through interlaminar damage and the friction between the sub-layers and adhesive layers. Based on small contact stiffness about laminate plate, impact damage will be smaller than the experimental value, so that the absorbed energy will be smaller about 6.36% than the experimental value.

Figure 5 is stress clouds in different cohesive layers. The red areas indicate complete failure; the green portion represents part of the damaged area which is delamination progression areas; lighter color indicates the smaller degree of damage. It is seen from the figure 5 that the impact damage occur from the upper adhere layer. The delamination damage area of bottom layer is larger than the upper layer. The reason for this is the bottom adhere layer served under the bending stress which caused by the impact. Figure 6 shows the delamination damage growth images in adhere layers. The delamination damage area increased with the increase of time. In different adhere layer, for example the 5^{th} layer, the stratified area like peanut shells and damage layered area is approximately $60mm^2$. All those phenomena agree with the experimental data. The method of this research can be applied in composite structure design and life prediction.

Acknowledgements

The authors thank “Natural Science Foundation of Shandong Province, China” （Grant No. ZR2012EEM003) and “The Fundamental Research Funds for the Central Universities” (Grant No. HIT. NSRIF. 2013128) for the financial support for this project, and the referees for their valuable comments.

References

Matzenmiller, A., Lubliner, J. and Taylor, R. L. A. (1995), Constitutivemodel for anisotropic damage in fiber-composites. Mechanics of Materials , 20(2), pp. 125-152.

Hou , J. P., Petrinic, N., Ruiz, C. and Hallett, S. R. (2000), Prediction of impact damage in composite plates. Composites Science and Technology, 60, pp. 273- 281.

Zerbst, U. and Heinimann, M. (2009), Fracture and damage mechanics modelling of thin-walled structures. Engineering Fracture Mechanics, 76, PP. 5-43.

Karim, M. R. (2005), Constitutive modeling and failure criteria of carbon-fiber reinforced polymers under high srain rate.USA: University of Akron.

Hou, J. P., Petrinic, N., Ruiz, C. and et al. (2000), Prediction of impact damage in composite plates. Composite Science and Technology, 60(2), pp. 273-281.

Sebastian, Heimbs. And Sven, Heller.(2008), Simulation of Low Velocity Impact on Composite Plates with Compressive Preload. Material Ⅱ- Composites , Copyright by DYNAmore Gmbh.

Masaaki, N. and Tomonaga, O. (2007), Numerical simulation of interlaminar damage propagation In CFRP cross-ply laminates under transverse loading. Solids And Structures, 44, pp. 3101-3113.

Shi, Y., Swait, T. and Soutis, C. (2012), Modelling damage evolution in composite laminates subjected to low velocity impact. Composite Structures, 94, pp. 2902-2913.

Schon , J. (2000), Coefficient of friction of composite delamination surfaces. Wear, 237, pp. 77-89.